

Misorientation angle dependence of bicrystal magnetoresistance within the model of coherent rotation

This article has been downloaded from IOPscience. Please scroll down to see the full text article.

2004 J. Phys.: Condens. Matter 16 3761

(<http://iopscience.iop.org/0953-8984/16/21/024>)

View [the table of contents for this issue](#), or go to the [journal homepage](#) for more

Download details:

IP Address: 129.252.86.83

The article was downloaded on 27/05/2010 at 14:58

Please note that [terms and conditions apply](#).

Misorientation angle dependence of bicrystal magnetoresistance within the model of coherent rotation

R Gunnarsson¹ and M Hanson²

¹ Department of Microtechnology and Nanoscience, Chalmers University of Technology, SE-412 96 Göteborg, Sweden

² Department of Experimental Physics, Chalmers University of Technology, and Göteborg University, SE-412 96 Göteborg, Sweden

E-mail: robert.gunnarsson@mc2.chalmers.se

Received 30 March 2004

Published 14 May 2004

Online at stacks.iop.org/JPhysCM/16/3761

DOI: 10.1088/0953-8984/16/21/024

Abstract

Bicrystal magnetoresistance hysteresis is studied within the model of coherent rotation of magnetization. The magnetoresistance hysteresis is calculated numerically in the limit of fully spin polarized current for symmetric bicrystal junctions with biaxial magnetic anisotropy and of varying misorientation angles. The shape of the curves obtained from the model displays different characteristic features, depending on the angular relationships, which are consistent with experimental data from the literature. The results show a magnetoresistance increasing with increasing misorientation angle. The influence of biaxial magnetocrystalline anisotropy is reflected in a hump in the maximum magnetoresistance curve at around a misorientation angle of 25°. This structure is absent in the case of uniaxial anisotropy.

1. Introduction

Spin polarized transport in magnetic tunnel junctions is the subject of a large bulk of recent scientific studies. A simple magnetic tunnel junction consists of two uniformly magnetized ferromagnetic electrodes separated by a non-magnetic barrier, a type of device that can be realized as, e.g., point contacts or planar junctions [1]. The by far most used measure of the quality of a magnetic tunnel junction is its tunnelling magnetoresistance (TMR) response. The formula of Julliere [2] has been applied to extract the spin polarization of the device from the TMR magnitude. Systems with high spin polarization have high TMR values and thus are promising candidates for high sensitivity magnetic field sensor or low power memory

applications. Ideal materials for magnetic tunnel junction electrodes would be half-metallic ferromagnets, which yield completely spin polarized currents.

A problem in most junctions is controlling the orientation of the magnetocrystalline anisotropy with respect to the magnetic field. This can be solved by using bicrystals, i.e. two single crystals sintered together with their crystalline axes oriented to form a grain boundary with a well defined misorientation angle. Traditionally such systems were used to form Josephson junctions in high temperature superconductors [3]. Bicrystal junctions were created also in ferromagnetic perovskite manganites [4] and, interestingly, half-metallic properties were observed in manganites [5]. Studies on single manganite bicrystal junctions [6–9], as well as on arrays of bicrystal junctions [4, 10–12] simulating the behaviour of polycrystalline manganites, were presented. Furthermore, the gradual change in TMR hysteresis from a single manganite bicrystal grain boundary to a 100-junction grain boundary array was demonstrated [13].

The experimental studies consistently show that the character of the TMR hysteresis depends crucially on the direction of the applied magnetic field [7–10, 13]. With the field applied parallel to the grain boundary ($B \parallel \text{GB}$) the magnetization reversal process is dominated by domain wall nucleation, motion and annihilation. The magnetoresistance in that configuration is stepwise for single junctions, revealing a stochastic magnetization reversal process. The magnetoresistive behaviour in the case of the magnetic field applied perpendicular to the bicrystal interface ($B \perp \text{GB}$) is completely different. With $B \perp \text{GB}$ the magnetoresistance of a single junction is smooth and shows a distinct switching field [9, 13]. This reveals the importance of the underlying processes of magnetization reversal for the magnetoresistive behaviour of tunnel junction devices.

Recently it was shown that in the $B \perp \text{GB}$ configuration the observed bicrystal magnetoresistance hysteresis can be analysed within the Stoner–Wohlfarth model for coherent rotation of the magnetization direction [9, 14]. A similar analysis was made by García and Alascio [15] where they applied a uniaxial Stoner–Wohlfarth model to analyse the magnetoresistance response.

In this paper we will analyse the dependence of the magnetoresistance upon the misorientation angle for bicrystal junctions within a model for coherent rotation. The paper is organized as follows. First the models for magnetization reversal and spin polarized transport are presented. Then the results of the numerical simulations are presented and discussed. Finally, a brief review of the experimental data provided in the literature and a comparison to what is obtained from the numerical calculations are given.

2. Model

Consider a two-dimensional case (as for a thin film) with magnetic electrodes, or grains, in the x – y plane, as shown schematically in figure 1. The two grains (denoted as left and right), both with in-plane magnetization, but with separate easy directions of magnetization at an angle α with the barrier, are subject to a magnetic field applied along the x -axis. In a first approximation the magnetic coupling between the grains is considered weak, even though there is a channel for a spin polarized current to flow between the left and the right electrode. The grain boundary magnetoresistance is a result of the dependence of the conductivity on the magnetic field. Hence, a proper model for the angular dependence of the magnetoresistance must include both the direction of magnetization as a function of magnetic field and the accompanying impact on the conductivity.

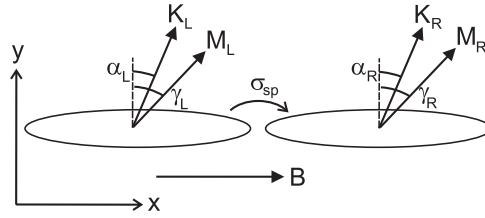


Figure 1. We consider the two-dimensional case: two electrodes with a channel for spin polarized electrons, but magnetically separated by a barrier along the y -direction, have their easy directions of magnetization, indicated by K , at different angles to the barrier. M is the magnetization in a magnetic field applied along the x -direction.

2.1. Magnetization reversal

The direction of the magnetization in a grain can be found from micromagnetic calculations including exchange, magnetocrystalline, magnetostatic and Zeeman energy contributions (see, e.g., [16]). In a homogeneously magnetized grain, decoupled from the surroundings and with negligible in-plane shape anisotropy, only the magnetocrystalline and Zeeman terms contribute to the angular variation of the energy. Hence, the magnetic energy density of grain i can be written as

$$\omega = \frac{K}{4} \sin^2 2(\alpha_i - \gamma_i) - MB \cos(\pi/2 - \gamma_i), \quad (1)$$

where K is the (first-order) biaxial anisotropy coefficient, M the saturation magnetization and γ the angle between the magnetization direction and the grain boundary ($i = \text{left, right}$). The applied field is perpendicular to the grain boundary. In this model we do not allow for domains to form and hence the reversal process will be through coherent rotation of magnetization.

In a dc magnetoresistance experiment K , α and the magnitude of M are kept constant. As B is changed slowly, which in this model means that we consider the static case, the direction of magnetization can be found from local minima in equation (1). Starting at saturation in a high magnetic field, where the Zeeman energy dominates and ω has a single (global) minimum, one can find $\gamma(B)$ by tracing the local minimum as it evolves with decreasing B . This is illustrated in figure 2, showing energy versus angle of magnetization (γ) curves obtained from equation (1) for a series of values of the reduced magnetic field BM/K .

The system considered here includes two grains with their easy axes in different directions α_L and α_R .⁴ Energy minimization for each side separately yields $\gamma_L(B)$ and $\gamma_R(B)$. In this paper we restrict the analysis to *symmetric* grain boundaries where $\alpha_L = -\alpha_R$. In figure 3 (left column) the angle of magnetization is shown for different misorientation angles. Due to the symmetry, the two sides of the junction simultaneously switch their magnetization directions.

2.2. Electron transport

We consider only the spin polarized conductivity contribution in the limit of direct tunnelling between two misoriented grains. A model for direct tunnelling between two ferromagnets with different directions of magnetization is given by Slonczewski [17]. By matching the free electron wavefunctions for the left and the right side he found the magnetic valve conductance $G = G_0(1 + P^2 \cos(\gamma_L - \gamma_R))$, where G_0 is the junction mean surface conductance and P the effective spin polarization of the ferromagnet–barrier system. The spin polarized contribution

⁴ The total misorientation angle of the grain boundary is defined as $|\alpha_L| + |\alpha_R|$.

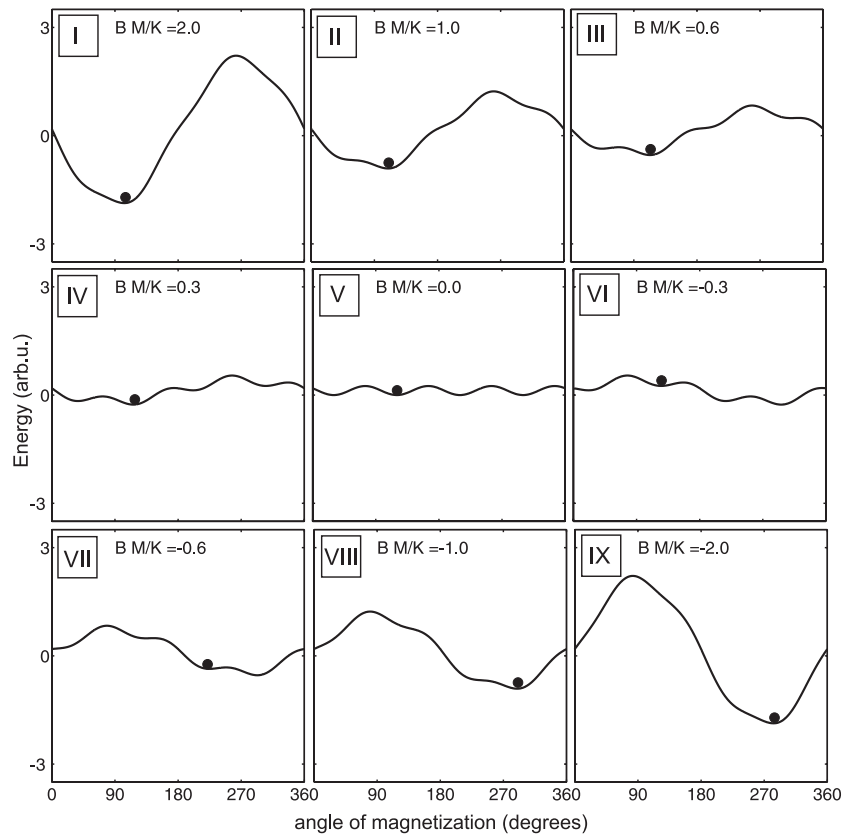


Figure 2. Calculated magnetic energy versus angle of magnetization in a crystal grain with $\alpha = 30^\circ$. In a field sweep from positive saturation to negative (frames I to IX) the local minima are indicated by the small ball.

to the junction resistance will then be

$$R \propto \frac{1}{1 + P^2 \cos(\gamma_L - \gamma_R)}. \quad (2)$$

Hence, through the magnetic field dependence of γ , the magnetoresistance $R(B)$ of the junction can be obtained. No other magnetic field dependent conductivity contributions, such as spin-flip scattering, are considered. In the calculation of the magnetoresistance the value of $P = 1$, corresponding to ideal half-metallic ferromagnetic grains, is used.

3. Magnetoresistance dependence on misorientation angle

Numerically calculated magnetoresistance curves, normalized to the zero-field value, are shown in the right column of figure 3 for the symmetric misorientation angles $10^\circ/10^\circ$, $20^\circ/20^\circ$, $25^\circ/25^\circ$, $30^\circ/30^\circ$ and $40^\circ/40^\circ$. The general behaviour is the same for all angles: initially the magnetoresistance increases smoothly and then suddenly falls off to low values again. The details in the shape of the hysteresis are determined by the angle of magnetization γ for the left and right sides. This angle is, in turn, determined by the evolution of the energy minima calculated from equation (1). For low values of α the magnetization switching results in a single

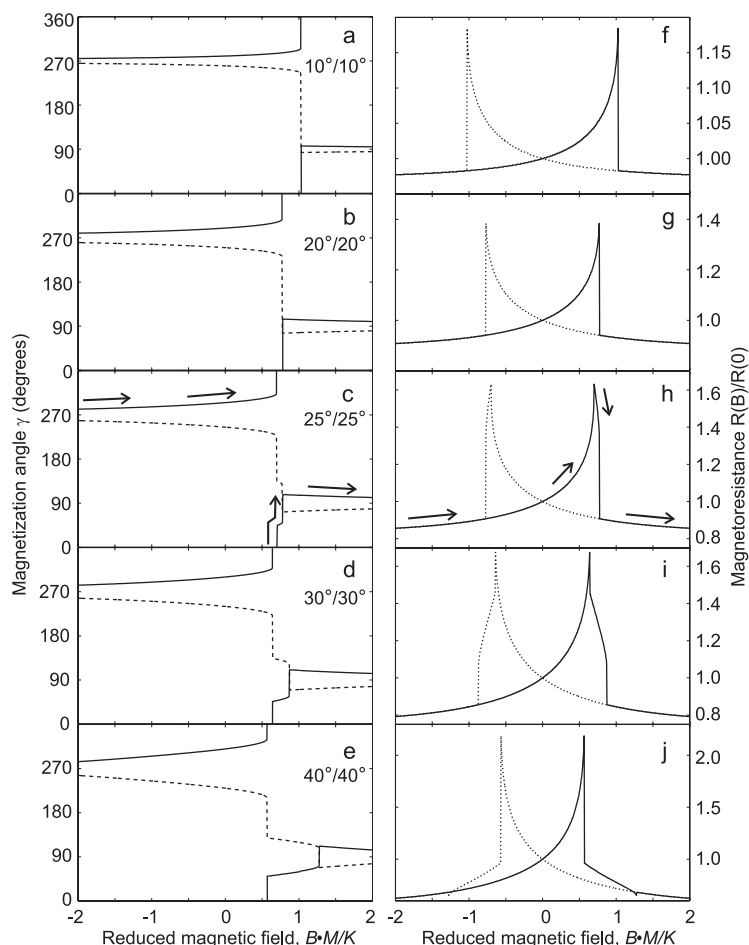


Figure 3. ((a)–(e)) Angle of magnetization γ for the left (dashed curves) and right (solid curves) grains as the magnetic field is swept from negative to positive values (the field sweep direction is indicated by arrows). ((f)–(j)) Corresponding magnetoresistance hystereses. The curves from top to bottom are calculated for increasing symmetric misorientation angles, as noted in the figure. Note the different scales for the magnetoresistance.

sharp peak in the magnetoresistance, figure 3(f). At around $\alpha = 23^\circ$ a shoulder appears just after the maximum magnetoresistance has been reached; cf figure 3(h). This shoulder is a result of the biaxial magnetocrystalline anisotropy, not present in the case of uniaxial anisotropy, and its appearance can be understood by considering the energy diagram. In moderate magnetic fields ($BM/K \approx 0.6$ for $\alpha = 30^\circ$) there exist two local minima (panel VII in figure 2), and coming from a higher energy state the magnetization rotation can be momentarily paused in such a minimum. As the magnetic field increases further, the two minima collapse into one (panel VIII in figure 2). For increasingly larger misorientation angles ($\alpha > 30^\circ$) the shoulder gradually decreases, figure 3(j), and as α approaches 45° the hysteresis reassumes the single-peak shape obtained for low angles, now with a switch that occurs for lower fields.

It is not only the shape of the magnetoresistance curve that changes with increasing misorientation angle: its magnitude also varies. In the present model the maximum magnetoresistance is determined by the angular difference between the magnetization

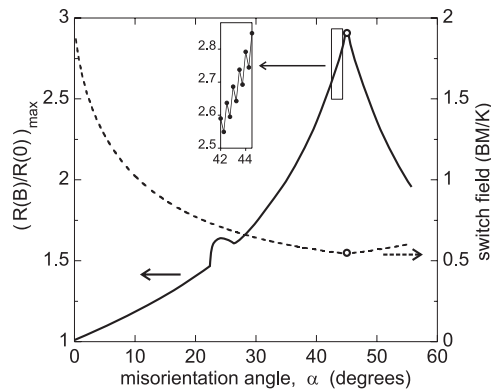


Figure 4. Angular dependence of the bicrystal TMR peak: the magnitude (solid curve) and switching field (dashed curve). The solid curve is a fit to the simulated data. The inset shows a discretization artefact at high misorientation angles. Both the TMR magnitude and switching field curves are discontinuous at $\alpha = 45^\circ$, indicated by open circles.

directions at the point where the local minimum turns into a terrace point in the energy diagram. In the case of $\alpha = 30^\circ$ this happens at about 0.6 BM/K . The peak value increases continuously with increasing misorientation angle. In figure 4 the maximum magnetoresistance $(R/R(B=0))_{\text{max}}$ is shown as a function of misorientation angle in symmetric junctions. The diagram is drawn for angles up to 55° . In a biaxial system it is only meaningful to discuss symmetric misorientation angles up to 45° , and thus the range from 45° to 90° is symmetric to the graph between 0° and 45° . Figure 4 also shows the switching field. We find that the model predicts that for pure spin dependent tunnelling the switching field decreases with increasing misorientation angle.

In a numerical simulation, the value of the magnetoresistance maximum naturally depends on the actual discretization of the magnetic field. At high misorientation angles an artefact could be observed when coarse steps were used; see the inset in figure 4. However, more interesting to note: there is a hump in the maximum magnetoresistance as a function of misorientation angle at around $\alpha = 25^\circ$ (23° – 27°), which is not a numerical artefact. The appearance of this feature coincides with that of the shoulder in the magnetoresistance curve discussed above. A closer examination of figures 3(c) and (d) reveals that just after the main switch of the magnetization direction, the difference $\gamma_L - \gamma_R$ is actually *larger*, thus leading to a higher magnetoresistance, than immediately before.

In the case of asymmetric grain boundaries, that is, e.g., $0^\circ/45^\circ$, the angular dependence is more intricate. The switching events in asymmetric junctions are not simultaneous in B . As a result of this, for some misorientation angles, one of the electrodes can be reversed, while the magnetization in the counter-electrode remains basically unaltered. Bringing it to the extremum, this scenario causes an infinite resistance. In a real experiment, however, the resistance will be limited by additional non-spin polarized current contributions and spin-flip processes.

4. Comparison with experiments

A few sets of experimental data were presented on bicrystal manganites, in which the field was applied perpendicular to the grain boundary and thus the magnetoresistance hysteresis could be analysed in terms of coherent rotation of the magnetization [4, 7–11, 13]. Systematic

studies of the influence of the misorientation angle are scarce: among the studies referred to, only Isaac *et al* [11] include a series of different bicrystals. However, in the following we discuss the experimental observations in relation to the present model, as regards the shape and character of the magnetoresistance curves, as well as the switching field.

Single values of bicrystal angles were previously studied by a few groups [7–9, 13]. Low angle junctions were studied in [13], where a $4.4^\circ/4.4^\circ$ LaAlO_3 bicrystal was employed as a template for $\text{La}_{0.67}\text{Sr}_{0.33}\text{MnO}_3$ microbridges. The magnetoresistance hysteresis showed two single peaks (one for increasing field and one for decreasing field), with a hysteresis shape similar to what can be expected for low angle bicrystal junctions; cf figure 3(f).

Philipp and co-workers [7] demonstrated well defined bicrystal magnetoresistance hysteresis in $\text{La}_{1-x}\text{Ca}_x\text{MnO}_3$ ($x = 0.3$) microbridges on symmetric SrTiO_3 bicrystals with a misorientation angle of $12^\circ/12^\circ$. Todd *et al* [8] studied the thickness dependence of the same kind of material with $22.5^\circ/22.5^\circ$ misorientations. Both groups obtained a similar behaviour of the magnetoresistance in such junctions, with the field applied perpendicular to the interface. Furthermore, the same general features were observed also by Gunnarsson *et al* [9] in a Sr-doped manganite $15^\circ/15^\circ$ bicrystal grown on SrTiO_3 , even though the magnetoresistance in the latter case yields a slightly more rounded hysteresis. The three studies are in reasonable agreement with the shape of the magnetoresistance hysteresis for $\alpha = 30^\circ$; cf figure 3(i)⁵. We especially note that all three sets of data [7–9] consistently show a smoothly increasing magnetoresistance, a shoulder after the maximum and a sudden drop to the same level as for the increasing magnetoresistance with the reversed field sweep direction. The field ranges of the shoulder are different for the three studies, ranging from 20 mT [9] and 100 mT [8] to 200 mT [7], which can be understood considering the difference in magnetocrystalline anisotropy and magnetization for the different devices.

A bicrystal grain boundary array was studied in a Wheatstone-bridge geometry by Mathur *et al* [4]. We note that in their paper the magnetoresistance hysteresis for junctions with $\alpha = 12^\circ$, that were subject to a field $B \perp \text{GB}$ at 77 K, has the character of the curve in figure 3(j). A similar sample was presented by Isaac *et al* [11]⁶, in which case the magnetoresistance hysteresis is more like the curve in figure 3(g). Also Steenbeck *et al* [10] studied a bicrystal grain boundary junction array. However, their magnetoresistance hysteresis in the $B \perp \text{GB}$ configuration does not exhibit the same type of sharp peaks as reported by the other groups. The reason for this difference is not yet clear, but it might be due to the formation of magnetic domains during switching.

Isaac *et al* [11] studied the influence of the misorientation angle on the magnetoresistance. They used Sr-doped manganite films grown on four SrTiO_3 bicrystals with different symmetric (total) misorientation angles: 4° , 24° , 36.8° and 45° . The magnetoresistance was measured at 300 and 77 K on a Wheatstone bridge meander geometry, containing 38 junctions. Isaac and co-workers normalized the resistance to the zero-field intersection of the extrapolated high field resistance, and found a close to linear relationship between the total misorientation angle and the maximum magnetoresistance. Comparing their result with what would be expected from a magnetization rotation process (figure 4) we find a reasonable agreement. The experimental data in that paper reach a highest total misorientation angle of 45° , equivalent to our $22.5^\circ/22.5^\circ$. This is just below the angles where the hump is observed in figure 4. Hence the existence of the hump cannot be confirmed by that experiment.

⁵ Keeping in mind that the easy axes of magnetization have been found to be in $\langle 110 \rangle$ directions for manganite materials [18, 19], the effective misorientation angles are virtually the same as (in our notation) $22.5^\circ/22.5^\circ$, $33^\circ/33^\circ$ and $30^\circ/30^\circ$, respectively.

⁶ The samples presented in [4] and [11] have the same layout, but the microbridges in [4] consist of 200 nm thick $\text{La}_{0.7}\text{Ca}_{0.3}\text{MnO}_3$, whereas the $12^\circ/12^\circ$ sample in [11] is based on a 100 nm thick Sr-doped manganite.

The switching fields are not readily extracted from the data in [11]. Thus, the dependence of the switching field on the misorientation angle, predicted by our model of coherent rotation and shown in figure 4, remains to be experimentally verified.

5. Conclusions

In this paper we studied the magnetoresistance hysteresis of bicrystal junctions in a magnetization reversal model of Stoner–Wohlfarth-like coherent rotation of the magnetization. The model applies when the field is perpendicular to the grain boundary of a bicrystal with biaxial anisotropy. The shape of the magnetoresistance hysteresis was calculated numerically in the limit of fully spin polarized current for symmetric bicrystal junctions. We found that in general the magnetization rotation results in a magnetoresistive response that increases with increasing field and falls abruptly at a well determined switching field. At high misorientation angles ($\geq 23^\circ$) a second jump appears in the magnetization rotation and the accompanying magnetoresistive hysteresis, which is reflected also in the angular dependence of the magnetoresistance magnitude. From the good agreement between the model calculations and the general features of the experimental observations we conclude that the low field magnetoresistance may be well described by the present coherent rotation model.

Acknowledgments

The work was financially supported by The Swedish Board for Strategic Research (SSF) and The Swedish Research Council (VR) within the programmes ‘OXIDE’ and ‘Microelectronics’, and ‘Transport in mesoscopic structures’, respectively.

References

- [1] See, e.g., Tsymbal E Y, Mryasov O N and LeClair P R 2003 *J. Phys.: Condens. Matter* **15** R109
- [2] Julliere M 1975 *Phys. Lett.* **54** A225
- [3] Hilgenkamp H and Mannhart J 2002 *Rev. Mod. Phys.* **74** 485
- [4] Mathur N D, Burnell G, Isaac S P, Jackson T J, Teo B-S, McManus Driscoll J L, Cohen L F, Evetts J E and Blamire M G 1997 *Nature* **387** 266
- [5] Park J-H, Vescovo E, Kim H-J, Kwon C, Ramesh R and Venkatesan T 1998 *Nature* **392** 794
- [6] Todd N K, Mathur N D, Isaac S P, Evetts J E and Blamire M G 1999 *J. Appl. Phys.* **85** 7263
- [7] Philipp J B, Höfener C, Thienhaus S, Klein J, Alff L and Gross R 2000 *Phys. Rev. B* **62** R9249
- [8] Todd N K, Mathur N D and Blamire M G 2001 *J. Appl. Phys.* **89** 6970
- [9] Gunnarsson R, Ivanov Z, Dubourdieu C and Roussel H 2004 *Phys. Rev. B* **69** 054413
- [10] Steenbeck K, Eick T, Kirsch K, Schmidt H-G and Steinbeiss E 1998 *Appl. Phys. Lett.* **73** 2506
- [11] Isaac S P, Mathur N D, Evetts J E and Blamire M G 1998 *Appl. Phys. Lett.* **72** 2038
- [12] Westerburg W, Martin F, Friedrich S, Maier M and Jakob G 1999 *J. Appl. Phys.* **86** 2173
- [13] Gunnarsson R, Kadigrobov A and Ivanov Z G 2001 *Mater. Res. Soc. Symp. Proc.* **674** U3.7
- [14] Gunnarsson R, Hanson M and Dubourdieu C 2004 *J. Appl. Phys.* at press *Preprint cond-mat/0404193*
- [15] García D J and Alascio B 2002 *Physica B* **320** 7
- [16] Aharoni A 2000 *Introduction to the Theory of Ferromagnetism (International Series of Monographs in Physics vol 109)* 2nd edn (Oxford: Oxford University Press)
- [17] Slonczewski J C 1989 *Phys. Rev. B* **39** 6995
- [18] Steenbeck K and Hiergeist R 1999 *Appl. Phys. Lett.* **75** 1778
- [19] Berndt L M, Balbarin V and Suzuki Y 2000 *Appl. Phys. Lett.* **77** 2903